A comparative multi-reference configuration interaction study of the low-lying states of two thione isomers of thiophenol

Filipe Belarmino de Lima,[1] Gessenildo Pereira Rodrigues,[2] Juracy Regis de Lucena Junior,[3] Elizete Ventura,[1] Rui Fausto,[4] Igor Reva,[4*] Silmar Andrade do Monte[1*]

[1]Departamento de Química, CCEN, Universidade Federal da Paraíba, 58059-900, João Pessoa-PB, Brazil

[2]Faculdade Rebouças, 58406-040, Campina Grande-PB, Brazil

[3]Departamento de Química, Universidade Estadual da Paraíba, 58429-500, Campina Grande-PB, Brazil

[4]Departamento de Química, Universidade de Coimbra, 3004-535, Coimbra, Portugal

*Corresponding authors: reva@qui.uc.pt, silmar@quimica.ufpb.br

Abstract. Multi-reference configuration interaction, MR-CI (including extensivity corrections, named +Q) calculations have been performed on S_0 to S_3 states of cyclohexa-2,4-diene-1-thione (thione**24**) and cyclohexa-2,5-diene-1-thione (thione**25**), which are thione isomers of thiophenol. Several types of uncontracted MR-CIS and MR-CISD wavefunctions have been employed, comprising MR-CI expansions as large as ~ 374 x 10^6 configuration state functions. The nature of the studied excited states has been characterized. Vertical excitation energies (ΔE) and oscillator strengths (*f*) have been computed. The most intense transitions ($S_0 \rightarrow S_2$ for **24** and $S_0 \rightarrow S_3$ for **25**) do not change with the wavefunction, although a variation as large as ~ 1 eV has been obtained for the S_3 state of **24**. On the other hand, ΔE changes at most ~ 0.15 eV for **25**, as the wavefunction changes. The S_1 state of both thiones has nπ* character and is in the visible region. For **24** S_2 and S_3 are ππ* and nπ* states, respectively, while for **25** the reverse order has been obtained. S_2 and S_3 are in the range from ~ 3.5 to 5.2 eV, at the highest level (MR-CI+Q). It is the first time that the excited states of the title molecules are studied. The computed results agree with the experimental onsets of photoreactions of thiones **24** and **25** found by Reva *et. al.* (*Phys. Chem. Chem. Phys.* **2015**, *17*, 4888).

Introduction

Cyclohexa-2,4-diene-1-thione (**24**; Figure 1) has been identified in a ground state isomerization reaction of thiophenol, studied at the MP2 and QCISD(T) levels by Al-Muhtaseb*et al.*[1] Those authors obtained a very large barrier of ~ 63 kcal/mol for the thiophenol → **24** thiol-thioneH-transfer reaction. Although formation of the analogous cyclohexa-2,5-diene-1-thione (**25**; see Figure 1) has also been studied, the authors did not find a direct pathway for formation of **25** from thiophenol.[1]

Reva *et. al.*[2] have isolated thiophenol in cryogenic argon matrices and observed the reversible photochemical thiophenol↔**24** and **24**↔**25** reactions. This was the first experimental observation ofthione isomers **24** and **25**. According to the authors, the direct thiophenol↔**25** photoisomerization reaction could not be discarded nor confirmed.[2]

In the present work the first three excited singlet states of **24** and **25** have been studied at the MR-CIS and MR-CISD levels, with inclusion of extensivity corrections (hereafter named +Q). Basis set effects were also taken into account. The results obtained for the two investigated systems were then used to address the excited states reached in the photochemical experiments performed by Reva *et. al.*[2] This is the first time that the excited states of thiones **24** and **25** are studied.

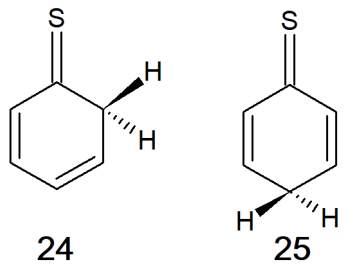

Figure 1. Thione isomers of thiophenol: cyclohexa-2,4-diene-1-thione (**24**, reads: "two-four") and cyclohexa-2,5-diene-1-thione (**25**, reads "two-five").

Computational Methods

The optimized structures of molecules **24** and **25** have been taken from ref.[2] (B3LYP/aug-cc-pVTZ data). Frequency calculations have also been performed in ref.[2], confirming that the obtained structures correspond to minima. Molecules **24** and **25** have C_s and C_{2v} symmetry, respectively.

In the present study, the active space used for thiones **24** and **25** at the CASSCF level consists of 12 electrons in 11 orbitals. Two A′ and two A″ states have been averaged at the CASSCF level for **24**, while for **25** one state for each one of the four symmetries (A_1, B_1, B_2 and A_2) has been averaged (in both cases with the same weights). For both systems these are the four lowest states at the CASSCF level. Due to the equivalence between the two C_{sp3}–H bonds of **24** and **25**, the σ orbitals in these molecules are equally localized on these bonds. Two pairs of active σ orbitals, the $\sigma_{C-H}/\sigma^*_{C-H}$ and $\sigma_{CS}/\sigma^*_{CS}$ pairs, have been included for both **24** and **25**. The C atom of the former pair is the sp^3 C atom, for both molecules (see *Figure* 1).

For **25**, three of the six active π orbitals are named $\pi_{CS}+\pi_{ring}$ (≡ π_1), n_π (≡ π_3, an essentially non-bonding S orbital) and $\pi_{C=C}$ (that is, mainly localized on the C=C bonds, named π_2). The other non-bonding S orbital, perpendicular to the previous one, is simply named *n*, and the three anti-bonding π orbitals are named $\pi^*_{CS}+\pi^*_{ring}$ (≡ π_1^*), $\pi_2^*{}_{C=C}$ (≡ π_2^*) and $\pi_3^*{}_{C=C}$ (≡ π_3^*).

For **24**, a non-bonding S orbital is again named *n* (as for **25**). The three bonding active π orbitals are named π_1, π_{CS} (≡ π_2) and $\pi_S+\pi_{C=C}$ (≡ π_3), while the anti-bonding orbitals are named $\pi_1^*{}_{ring}+\pi^*_{CS}$ (≡ π_1^*), $\pi_2^*{}_{ring}+\pi^*_{CS}$ (≡ π_2^*) and $\pi^*_{C=C}$ (≡ π_3^*).

The subscripts of theorbitals (such as $_{CS}$, $_{C=C}$, etc.) refer to their localization. Additional details can be found in the supporting information.

The $\sigma_{CH}/\sigma^*_{CH}$ pairs of **24** and **25** have been included in the active space (for most of the wavefunctions here used) as this study is the first step towards a description (on the same grounds) of photoinduced hydrogen migration pathways associated with the thiophenol→**24**, thiophenol→**25** and **24**→**25** reactions. Besides, the above mentioned active space was constructed considering also the following two reasons: (i) as some preliminary calculations at the CASSCF level performed for thiophenol showed that the $\sigma_{CS}/\sigma^*_{CS}$ pair should be included in the active space, due to its admixture with the $\sigma_{SH}/\sigma^*_{SH}$ pair, the former pair has also been included in the active spaces of **24** and **25** (for most of the wavefunctions here used), due to the thiophenol→**24** and thiophenol→**25** reactions,[2] which we intend to study; (ii) the highest level results for thiophenol (at the CASPT2 level, discussed later and compared to the results here obtained) include the eleven orbitals which transform into the eleven orbitals here used for **24** and **25**, along the thiophenol→**24** and thiophenol→**25** reaction pathways (as will be discussed elsewhere).

Four types of wavefunctions have been used in this work, named *w1*, *w2*, *w3* and *w4*. *w1* is an MR-CIS wavefunction, used for both systems, while the remaining are MR-CISD wavefunctions. *w2* and *w3/w4* are used for **25** and **24**, respectively. For *w2* the CAS space has been reduced, transferring strongly and weakly occupied orbitals to the doubly occupied (DOCC) and auxiliary (AUX) spaces, respectively, as discussed below, and for *w3* the CAS orbitals are split into reduced active space (RAS) and auxiliary (AUX) orbitals. It was not possible to use *w3* for **25**, as in this case single occupied → anti-bonding excitations are not enough to generate the correct number of guess vectors for each irreducible representation. In the case of *w4* the four σ orbitals have been removed from the CAS (at both CASSCF and MR-CI levels) and the *n* and π_1 orbitals (24a′ and 3a″, respectively, see the supporting information) have been transferred to the RAS space, and only single RAS → CAS excitations are allowed while generating the reference configuration state functions (CSFs), yielding a set of reference CSFs based on a CAS(4,5) + single RAS → CAS excitations. Additional details concerning how these four wavefunctions are formed are given in Table 1.

w2 is the largest MR-CISD wavefunction here used (see Table 1) and has only been employed for **25**, due to its higher (C_{2v}) symmetry (see Figure 1), but at the expense of a reduced number of active orbitals. This reduction consists of transferring former active orbitals, namely, two bonding (σ_{CS} and σ_{CH}) and three anti-bonding orbitals (σ_{CS}*, σ_{CH}* and $\pi_3{}^*_{C=C}$, see supporting information) to the DOCC and AUX spaces, respectively, at the MR-CISD level.

The criteria chosen for these two sets of *w2* were: the active orbitals whose occupation numbers (nocc) are (at the CASSCF level) larger than 1.97 have been transferred to the DOCC space, while those with nocc< 0.1 have been transferred to the AUX space, and only single CAS → AUX excitations are allowed (yielding a set of reference CSFs based on a CAS(8,6) + single CAS → AUX excitations, see Table 1). One can check the importance of double internal → external excitations through a comparison between the results obtained from *w1* and *w2*. Ideally, for a more accurate comparison, *w2* should have the same complete active orbitals as *w1*. However, it is expected that *w2* already recovers a large fraction of the electron correlation of an MR-CISD wavefunction formed from a set of CAS(12,11) reference CSFs, due to the judicious choice of the previously active orbitals transferred to the DOCC and AUX spaces, as discussed above.

Table 1. Wavefunctions used in this work, at the MR-CI level.

Wavefunction	excitation levels used to generate the reference CSFs[a]	Internal → external[b] excitation level/final MR-CI wavefunction
w1	CAS(12,11)	singles/MR-CIS
w2	CAS(8,6) + single CAS→AUX excitations	singles and doubles/MR-CISD
w3[c]	single occ→anti-bonding excitations	singles and doubles/MR-CISD
w4	CAS(4,5) + single RAS → CAS excitations	singles and doubles/MR-CISD

[a]Configuration State Functions; [b]Internal corresponds to the set of doubly occupied + active + AUX orbitals, while external corresponds to the set of orbitals which are unoccupied (virtual) in the reference CSFs; [c]For *w3* occ comprises the subset of six orbitals (active at the CASSCF level) with the highest occupation numbers, while the anti-bonding subset comprises the five active orbitals with the smallest occupation numbers. For additional details concerning these orbitals see text and supporting information.

Due to the size of the system and to the basis sets used, multi-reference configuration interaction calculations with single and double excitations (MR-CISD) are only feasible for **24** with a large reduction of the number of reference CSFs, at least for uncontracted MR-CI wavefunctions (as discussed later). Such reduction has been applied to yield the wavefunctions *w3* and *w4*(see Table 1). The first one has been devised with the purpose to see what is the net effect of reducing the internal excitation level (in other words, splitting the CAS into RAS + AUX orbitals) but at the same time increasing the internal → external excitation level, yielding an MR-CISD wavefunction. *w3* has a similar size to that of *w1*. Again, due to the size of the system, an internal excitation level larger than one (between the occ and the anti-bonding subsets described in Table 1), combined with single and double internal → external excitations (yielding a MR-CISD wavefunction), is computationally prohibitive for **24**. However, the relatively small number of active orbitals used in *w4* allows all excitations compatible with a CAS(4,5). Besides, as explained before, additional reference CSFs are also generated through RAS → CAS excitations (see Table 1). *w4* corresponds to the largest CI expansion used for **24**.

Once the reference CSFs were formed, they were used to generate the excited CSF through single excitations from all internal into all external orbitals, at the MR-CIS level (for *w1*, see Table 1), and through single and double internal → external excitations at the MR-CISD level (for *w2*, *w3* and *w4*, see Table 1). The final CSF space is formed by the reference along with the excited CSFs.

There are two subsets of low-lying orbitals at the ground state geometries, the frozen core (FC) and the doubly occupied valence orbitals, at the MR-CIS/MR-CISD levels. The FC subset comprises the K (for the C atom) and K + L (for the S atom) shells. Such choice for the FC is based on the essentially correct description of the excited states of other systems containing another third row atom, Cl, at the MR-CISD level.[3,4,5,6,7,8,9,10] The difference between doubly occupied and FC orbitals is that, while the former set remains doubly occupied only in the reference CSFs, the latter is kept as so in the reference as well as in the excited CSF space. The multireference extension of the Davidson correction (+Q) has been used to take the size-extensivity error into account.[11,12] The interactive space restriction[13] has been used for *w2* and *w4* (see Table 1). All CASSCF, MR-CISD, and MR-CISD+Q calculations have been performed with the COLUMBUS program system.[14,15,16,17] The atomic orbitals (AO) integrals used by COLUMBUS have been computed with the DALTON program.[18] The aug-cc-pVTZ and the mixed aug-cc-pVDZ(C,H)/aug-cc-pVTZ(S) basis sets have been used in this study.[19,20,21]

Results and discussion

Basis set effect

The basis set effect has been taken into account at the CASSCF level, for both systems (see Table 2), and at the *w1* level for **25** (see Table 3). As it can be seen from Tables 2 and 3, the ΔE values obtained with both basis sets differ by at most 0.03 eV. Besides, the main configurations obtained for all four states do not change with the basis set, and the differences between their weights are virtually negligible, at both CASSCF and *w1* levels. Therefore, the results shown in Tables 2 and 3 give us confidence about the reliability of the aug-cc-pVDZ(C,H)/aug-cc-pVTZ(S) basis set towards the computationally much more demanding aug-cc-pVTZ(C,H,S) basis set.

Table 2. ΔE values (in eV) and configuration weights computed at the CASSCF level with the aug-cc-pVDZ(C,H)/aug-cc-pVTZ(S) basis set, for **24** and **25**thione isomers.

24			**25**		
State	ΔE	configurations[a,b]	State	ΔE	configurations[a,b]
$1^1A'$	0.00	0.60gs +0.25$\pi_3\pi_1$*	1^1A_1	0.00	0.80gs + 0.11$n_\pi\pi^*_1$
$1^1A''$	2.09 (2.07)[c]	0.80nπ_1*	1^1A_2	2.34 (2.31)[c]	0.90nπ_1*
$2^1A'$	4.50 (4.49)[c]	0.21$\pi_2\pi_1$* + 0.19$\pi_3\pi_1$* + 0.15$\pi_3^0\pi_1^{*2}$ + 0.12$\pi_3\pi_2$*	1^1B_1	4.91 (4.88)[c]	0.67nπ_2* + 0.20$n^1\pi_2{}^1\pi_1^{*2}$
$2^1A''$	4.55 (4.53)[c]	0.44nπ_2* + 0.23$n^1\pi_3{}^1\pi_1^{*2}$ + 0.12$n^1\pi_2{}^1\pi_1^{*2}$	1^1B_2	5.27 (5.25)[c]	0.42$n_\pi\pi_2$* + 0.25$\pi_2{}^1n_\pi{}^1\pi_1^{*2}$ + 0.21$\pi_2\pi_1$*

[a] gs stands for the ground state configuration; only configurations with weights larger than 0.1 are shown; [b]Configurations a^0b^2 and $a^1b^1c^2$ correspond to the a→b and (a,b)→c double excitations, respectively, and the remaining configurations correspond to single excitations; [c]Results obtained with the aug-cc-pVTZ(C,H,S) basis set. The weights obtained with both basis sets differ by at most 0.01.

Vertically excited states of 24 and 25

ΔE values, configuration weights and oscillator strengths (*f*) computed with *w1* and *w2* for **25** are shown in Table 3. As it can be seen through comparison between Tables 2 and 3, inclusion of dynamic electron correlation (at both MR-CIS and MR-CISD levels) slightly decreases the ΔE values, by at most 0.21 eV. A further decrease in the ΔE values is obtained upon inclusion of extensivity correction, but the effect is smaller than that of the dynamic electron correlation, leading to a maximum decrease of 0.1 eV. The nature of all studied states is the same, at the CASSCF and MR-CI levels (compare Tables 2 and 3). It is important to point out the non-negligible contribution of configurations formed by double excitations to the π_1* orbital, in the 1^1B_1 and 1^1B_2 states, although these weights decrease upon inclusion of dynamic electron correlation (compare Tables 2 and 3).

An important difference between the results obtained for thione isomers **24** and **25** and those obtained for the thiol isomer (thiophenol) is the absence of configurations formed by excitations to the σ* orbital, a feature observed for the S_2 state of thiophenol.[22,23,24,25,26] However, such difference is expected, as in thiophenol this orbital is localized on a considerably weaker (S–H) bond.

Using the CASPT2/aug-cc-pVTZ results for thiophenol as reference[22] (4.3, 4.5 and 5.1 eV for the S_1, S_2 and S_3 states, respectively), one can see a decrease in the excitation energies

(as one goes from thiophenol to **25**), with the largest effect obtained for the first excited state, followed by the second excited state. Compared to the highest level *w2*(+Q) results (as discussed later), the decrease for S_1 is as large as ~ 2.1 eV, while for S_2 is only ~ 0.3 eV, at the same level. For S_3 the changes are almost negligible, at both *w1*(+Q) and *w2*(+Q) levels (see Table 3)**.**

It is interesting to point out the change of nature of S_1 of the thione isomer **25** as compared to the thiol form of thiophenol. Although there is some contribution of the *n* orbital (perpendicular to the π systemof the ring) to the σ_{SH} and σ_{SC} orbitals of thiophenol,[23] configurations containing excitations from these orbitals are absent in the lowest four excited states of thiophenol.[22,23,24,25,26] On the other hand, in **25** (and also in **24**,as discussed later) the *n* orbital is very well localized (as shown in the supporting information). While in thiophenol S_1 is a ππ* state, in **25** it is an nπ* state (see Table 3). S_2 is also an nπ* state, and S_3 is a ππ* state (see Table 3). Thus, only the nature of S_3 is the same both in thiophenol[22] and in the thione isomer **25**.

The first excited state of **25** (1^1A_2) is in the visible region (with ΔE = 2.17 or 2.23 eV, at the *w1*(+Q) and *w2*(+Q) levels, respectively), but the $1^1A_1 \rightarrow 1^1A_2$ transition is dipole forbidden, by symmetry. However, the experimental threshold required for photochemical transformations of **25**, λ < 332 nm (3.73 eV), is consistent with a transition within the first band (see Table 3). Therefore, some intensity gain is expected to be taking place around 3.73 eV, due to vibronic and/or spin-orbit coupling mechanisms. Besides, one cannot rule out some intensity borrowing from the nearby $S_0 \rightarrow S_2$ transition.

Due to the judicious choice of the CASSCF active orbitals to be transferred to the DOCC and AUX spaces while forming the reference set of CSFs for *w2* (see Table 1 and the previous discussion concerning the criteria used for this transfer), it is expected that *w2* already recovers a large fraction of the electron correlation of an MR-CISD wavefunction formed from a set of CAS(12,11) reference CSFs. Consequently, the results obtained with *w2* can be considered the most reliable ones for **25**. As already mentioned, *w2* is the largest MR-CI wavefunction here employed, achieving ~3.8×10^8 CSFs.

From what has been said one can test the reliability of *w1* for **25** comparing its results with those obtained from *w2*. As it can be seen from Table 3, the computed excitation energies are very close, with a maximum difference of 0.13 eV, obtained for 1^1B_1 including extensivity corrections. The main configurations are maintained, for *w1* and *w2*, and the

largest change obtained for the configuration weights is 0.11 (also for 1^1B_1), a value which can be considered relatively small. On the other hand, the effect on the *f* values, due to the change from *w1* to *w2*, is significant, with reductions down to ~ 52 and 45 % for 1^1B_1 and 1^1B_2, respectively (see Table 3). Despite such reduction, the $S_0 \rightarrow S_3$ transition remains the most intense one for both wavefunctions. Therefore, *w1* can be considered a good approximation to *w2* (a computationally much more demanding wavefunction).

ΔE values, configuration weights and oscillator strengths (*f*) computed with *w1*, *w3* and *w4* for **24** are shown in Table 4. It is clear that the effect of dynamic electron correlation is considerably larger for the ΔE values of **24** than for those of **25**, and the effect for the latter is slightly dependent on the state (compare Table 2 with Tables 3 and 4). On the other hand, for **24** the effect of dynamic electron correlation is highly dependent on the state and on the wavefunction. For instance, as for the $2^1A'$ (S_2) state computed with *w1* a reduction of 0.68 eV is obtained, for the same state calculated with *w3* and *w4* one has reductions of only 0.24 and 0.19 eV, respectively, upon inclusion of dynamic electron correlation. However, in the case of the fourth state ($2^1A''$) a much larger reduction is obtained for *w3*, as compared to that obtained for *w1* (0.92 versus0.23eV). In contrast, for *w4* one has a slight increase of 0.28 eV (compare the CASSCF and MR-CI results from Tables 2 and 4, respectively).

Albeit the nature of the excited states (that is, nπ* or ππ*) of **24** does not change upon inclusion of dynamic electron correlation, the multiconfigurational character of S_2 and S_3 decreases significantly as dynamic electron correlation is included (compare Tables 2 and 4).

In the case of the S_1 state of **24** and **25** the effect of extensivity correction is similar and small, changing the ΔE values by at most 0.05 (for *w1* with the aug-cc-pVDZ(C,H)/aug-cc-pVTZ(S) basis set) and 0.12 eV (for *w4*), for **25** and **24**, respectively. For the S_2 and S_3 states of **24** the effect is significantly larger, decreasing the ΔE values of S_2 in a range from 0.20 to 0.28 eV, and those of S_3 from 0.10 to 0.22 eV (see Table 4).

It is important to point out that, even considering only single internal → external excitations from the reference CSFs generated at the CAS(12,11) level (as in *w1*, see Table 1), for **24** the final number of CSFs is already very large, ~ 2.1×10^8 CSFs, due to the system size, number of active orbitals and basis set. Therefore, if one includes single and double excitations, the calculation becomes computationally prohibitive, at least for an uncontracted multi-reference CI wavefunction, which is the type of MR-CI wavefunctions used in this

work.[27] The same can be said even if one uses the same type of active space reduction based on the CASSCF occupation numbers, as it has been done for the wavefunction *w2* of **25**.

Table 3. ΔE values (in eV), configuration weights and oscillator strengths (*f*) computed for **25**, at the *w1* and *w2* levels (see Table 1), with the aug-cc-pVDZ(C,H)/aug-cc-pVTZ(S) basis set. Multireference extension of the size-extensivity Davidson correction is indicated by (+Q).

States	Wavefunction *w1*				Wavefunction *w2*			
	ΔE	ΔE(+Q)	$f(\times 10^3)$	configurations[a,b]	ΔE	ΔE(+Q)	$f(\times 10^3)$	configurations[a,b]
1^1A_1	0.00	0.00	--	0.75gs	0.00	0.00	--	0.67gs
1^1A_2	2.23 (2.21)[c]	2.18 (2.17)[c]	--[d]	$0.82n\pi_1*$	2.20	2.23	--[d]	$0.75n\pi_1*$
1^1B_1	4.73 (4.71)[c]	4.63 (4.61)[c]	1.997	$0.69n\pi_2* + 0.10n^1\pi_2{}^1\pi_1*^2$	4.78	4.76	1.043	$0.58n\pi_2* + 0.15n^1\pi_2{}^1\pi_1*^2$
1^1B_2	5.10 (5.09)[c]	5.02 (5.01)[c]	16.628	$0.32\pi_2\pi_1* + 0.30n_\pi\pi_2* + 0.19n_\pi{}^1\pi_2{}^1\pi_1*^2$	5.06	5.03	7.493	$0.29n_\pi\pi_2*+ 0.24\pi_2\pi_1* + 0.21n_\pi{}^1\pi_2{}^1\pi_1*^2$

[a]gs stands for the ground state configuration; only configurations with weights larger than 0.1 are shown. The weights obtained with both basis sets (for *w1*) differ by at most 0.01; [b]Configurations $a^1b^1c^2$ correspond to the (a,b)→c double excitations, while the remaining configurations correspond to single excitations; [c]Results obtained with the aug-cc-pVTZ(C,H,S) basis set; [d]Forbidden by symmetry. For *w1* the total MR-CIS/MR-CIS+Q energies are (in au) –628.484673/–628.503650, and for *w2* the total MR-CISD/MR-CISD+Q energies are –629.066462/–629.221961.

Table 4. ΔE values (in eV), configuration weights and oscillator strengths (*f*) computed for **24**, at the *w1* and *w3* levels (see Table 1), with the aug-cc-pVDZ(C,H)/aug-cc-pVTZ(S) basis set. Multireference extension of the size-extensivity Davidson correction is indicated by (+Q).

States	Wavefunction *w1*				Wavefunction *w3*				Wavefunction *w4*			
	ΔE	ΔE(+Q)	$f(\times 10^3)$	configurations[a,b]	ΔE	ΔE(+Q)	$f(\times 10^3)$	configurations[a,b]	ΔE	ΔE(+Q)	$f(\times 10^3)$	configurations[a,b]
1^1A'	0.00	0.00	--	0.62gs + $0.19\pi_3\pi_1^*$	0.00	0.00	--	0.61gs + $0.16\pi_3\pi_1^*$	0.00	0.00	--	0.56gs + $0.16\pi_3\pi_1^*$
1^1A"	1.92	1.88	0.052	$0.79n\pi_1^*$	2.27	2.36	0.053	$0.77n\pi_1^*$	2.31	2.19	0.041	$0.73n\pi_1^*$
2^1A'	3.82	3.54	248.8	$0.54\pi_3\pi_1^*$ + 0.16gs	4.26	4.06	317.1	$0.53\pi_3\pi_1^*$ + 0.13gs	4.31	4.09	179.8	$0.32\pi_3\pi_1^*$ + $0.13\pi_2\pi_1^*$
2^1A"	4.32	4.22	0.061	$0.52n\pi_2^*$ + $0.18n^1\pi_3^1\pi_1^{*2}$	5.47	5.25	0.033	$0.76n\pi_2^*$	4.83	4.62	0.001	$0.46n\pi_2^*$ + $0.19n^1\pi_3^1\pi_1^{*2}$

[a]gs stands for the ground state configuration; only configurations with weights larger than 0.1 are shown; [b]Configurations $a^1b^1c^2$ correspond to the (a,b)→c double excitations, while the remaining configurations correspond to single excitations. For *w1*, *w3* and *w4* the total MR-CI/MR-CI+Q energies are (in au) –628.521163/–628.539777, –629.050072/–629.212969 and –629.073981/–629.225881, respectively.

One very important point is what type of wavefunction recovers a larger fraction of the electron correlation provided by a complete MR-CISD wavefunction, that is, an MR-CISD wavefunction based on a set of CAS(12,11) reference CSFs. As already mentioned, such type of calculation is not affordable, at least for an uncontracted wavefunction. However, one has two affordable options: (i) only single internal → external excitations, yielding an MR-CIS wavefunction (*w1*, see Table 1); (ii) an MR-CISD wavefunction based on reference CSFs generated through limited excitations among the internal orbitals (from the occ to the anti-bonding orbitals described in Table 1), as in the case of *w3* (for which only single occ → anti-bonding excitations have been applied, see Table 1). Though the answer concerning which type of wavefunction, *w1* or *w3*, recovers a larger fraction of the electron correlation provided by a complete MR-CISD wavefunction could not be obtained, one can compare the effect due to the change from *w1* to *w3* on the properties here studied for **24** (see Table 4). As case (ii) calculations based on higher than single excitations are not affordable, one could not study the effect of the excitation level (within the internal orbitalsgiven in Table 1) on the final properties. Instead, one can study the effect of removing the σ orbitals and, at the same time, increasing the excitation level within the active orbitals, through comparison between *w3* and *w4* (see Table 1).

As can be seen from Table 4, there are relatively large differences between the ΔE results obtained with *w1* and with the other wavefunctions, varying from 0.31 to 1.15 eV, and the maximum difference has been obtained for$S_3(2^1A'')$ either with or without extensivity corrections. On the other hand, the differences between the ΔEvalues obtained with *w3* and *w4*, for S_1 ($1^1A''$) and S_2 ($2^1A'$), are almost negligible (varying from 0.03 to 0.17 eV, see Table 4). For S_3 the differences between the *w3* and *w4* results are much larger (with values of 0.63 and 0.64 eV, with and without extensivity corrections, respectively, see Table 4). Therefore, it is clear that theΔE values obtained for S_3 shows by far the largest average variation among the wavefunctions (see Table 4), which can be taken as an evidence of the greater difficulty in describing this state.

Despite the relatively large differences between the ΔE values (especially for S_3, see Table 4), the nature of the states does not change with the wavefunction, even though there are some significant variations of the multiconfigurational character of S_2 and S_3 (see Table 4). Nevertheless, although the multiconfigurational character of S_2 is larger for *w4*, the weight of the ground state configuration is virtually negligible in this case, differently of what happens for *w1* and *w3* (see Table 4). For all three wavefunctions there are significant

contributions of the $\pi_3\pi_1^*$ configuration in the ground state wavefunction. For the S_3 state one has significant contributions of a double excitation ($n^1\pi_3^1\pi_1^{*2}$) only for *w1* and *w4*(see Table 4).

For all three wavefunctions the most intense transition of **24** remains the same ($1^1A' \rightarrow 2^1A'$, $S_0 \rightarrow S_2$, see Table 4). Based on the results obtained for the *f* values of **25** (and also based on the fact that **24** and **25** are similar), some decrease on the *f* values of **24** is to be expected (due to the change from *w1* to *w2*), if *w2* was not computationally prohibitive for **24**. However, it is not expected that the most intense transition changes. Such transition for **24** ($1^1A' \rightarrow 2^1A'$) is approximately 15 times more intense than that of **25** ($1^1A_1 \rightarrow 1^1B_2$, compare the *w1* results in Tables 3 and 4). This information, along with their corresponding excitation energies of 3.54 and 5.02 eV (obtained at the *w1*(+Q) level for **24** and **25**, respectively, see Tables 3 and 4), can be helpful if one wants to discriminate these two isomers through UV-VIS absorption spectroscopy.

By comparison between the CASPT2/aug-cc-pVTZ results for thiophenol, used as reference[22] (4.3, 4.5 and 5.1 eV for the S_1, S_2 and S_3 states, respectively), and those obtained for **24**, one can see how the ΔE values change in the thiophenol *vs.***24** pair. It is clear that the effect is by far the largest for S_1 (as in the thiophenol *vs.***25** pair). Comparing the CASPT2 results with the results obtained including extensivity corrections (+Q), the excitation energies of S_1 decrease by ~ 2.1 to2.4 eV, depending on the wavefunction (see Table 4). With exception of S_3 at the *w3*(+Q) level (where a slight increase of only 0.14 eV is obtained), the other ΔE(+Q) values of S_2 and S_3 decrease from 0.41 to 0.96 eV, depending on the state and on the level of theory used, again compared to the CASPT2 results (see Table 4).

The ΔE(+Q) values of S_1 (see Table 4), along with the computed *f* values (although very small), are in line with the observation from ref.[**Erro! Indicador não definido.**] that **24** is the only isomer which absorbs in the visible region. As discussed before, even if the first excited state of **25** is also in the visible region, its transition dipole moment vanishes by symmetry.

The experimental threshold for the photochemical transformations of **24** (λ< 427 nm = 2.90 eV) is consistent with excitation within the first band, associated with $1^1A''$ (an nπ* state; see Table 4).While in thiophenol S_1 is a ππ* state, in **24** it is an nπ* state, followed by an ππ*(S_2) and an nπ* (S_3) state (see Table 4). Thus, the nature of all three excited states change as one goes from thiophenol[22] to the thione isomer **24**. For **24** and **25** the most intense band is due to a transition to a $\pi\pi^*$ state, for all wavefunctions (see Tables 3 and 4).

Conclusions

The first four singlet states of thiones**24** and **25** have been studied using several types of uncontracted MR-CI wavefunctions, with the mixed aug-cc-PVDZ(C,H)/aug-cc-pVTZ(S) basis set. Excitation energies (ΔE), oscillator strengths (*f*) and nature of the excited states have been investigated. The basis set effect has also been taken into account. It is the first time that the excited states of **24** and **25** are studied.

The largest MR-CI calculation has been here performed for **25**, due to its C_{2v} symmetry, achieving ~ 3.8 x 10^8 CSFs. The change from thiophenol to **25** largely decreases the excitation energy of S_1 (based on previous CASPT2/aug-cc-pVTZ[22] and the ΔE(+Q) results, see Table 3). In the case of S_2, the effect is opposite but much smaller, increasing its excitation energy by at most 0.26 eV (at *w2*(+Q) level, see Table 3). In the case of S_3 the effect is almost negligible.

Although S_1 of **25** (1^1A_2) is in the visible region (with ΔE(+Q) ~ 2.2 eV, see Table 3), the $1^1A_1 \rightarrow 1^1A_2$ transition is dipole forbidden, by symmetry. The experimental threshold required for photochemical transformations of **25**, λ< 332 nm (3.73 eV[2]) is, according to our results, consistent with a transition within the first band. Therefore, some intensity gain is expected to be taking place around 3.73 eV, due to vibronic and/or spin-orbit coupling mechanisms. Intensity borrowing from the nearby band cannot be ruled out.

Only the nature of S_3 (a ππ* state) is maintained as thiophenol changes to **25**, with both S_1 (also a ππ* state) and S_2 (an $n_\pi\sigma^*$) excited states changing their nature to nπ*. On the other hand, for **24** the nature of the three first excited singlet states are nπ*, ππ* and nπ*, respectively. Thus, the nature of S_1 to S_3 change upon the thiophenol→**24** isomerization.

The ΔE values decrease largely with the thiophenol→**24** isomerization (again based on previous CASPT2/aug-cc-pVTZ[22] and ΔE(+Q) results), especially for S_1. The only exception is observed for S_3 with *w3* (see Table 4). The ΔE(+Q) values, along with the computed *f* values (although very small), are in line with the observation from ref.[2] that **24** is the sole isomer absorbing in the visible region. The experimental threshold for the photochemical transformations of **24** (λ< 427 nm = 2.90 eV) is consistent with excitation within the first band, associated with the $1^1A''$ (an nπ*) state.

Larger uncontracted MR-CI calculations still need to be performed (e.g., MR-CISD based on a set of CAS(12,11) reference CSFs), when they become computationally feasible, to see how the aforementioned results are affected. Alternatively, the effect of using more accurate extensivity corrections, as multi-reference average quadratic, MR-AQCC,might be evaluated in relation to alterations in the excited states' properties.[28]

Acknowledgements

I. R. acknowledges the Portuguese Foundation for Science and Technology (FCT) for an *Investigador FCT* grant. R.F. and I. R. thank FCT for financial support to the Coimbra Chemistry Centre (CQC, Research Unit UI0313/QUI/2019) co-funded by FEDER/COMPETE 2020-EU. E.V. thanks the Brazilian agency CNPq (Grant Number303884/2018-5 and 423112/2018-0) for support. The remaining authors are grateful to the Brazilian agencies CAPES and FINEP for financial support. They are also thankful to the CESUP/UFRGS supercomputing center for the computational facilities.

References

[1] A. H. Al-Muhtaseb, M. Altarawneh, M. H. Almatarneh, *J Comput.Chem.* **2011**, *32*, 2708. https://doi.org/10.1002/jcc.21852.
[2] I. Reva, M. J. Nowak, L. Lapinski, R. Fausto, *Phys. Chem. Chem. Phys.* **2015**, *17*, 4888. https://doi.org/10.1039/C4CP04125A.
[3] G. P. Rodrigues, T. M. L. de Lima, R. B. de Andrade, E. Ventura, S. A. do Monte, M. Barbatti, *J. Phys. Chem. A* **2019**, *123*, 1953. https://doi.org/10.1021/acs.jpca.8b12482.
[4] V. C. de Medeiros, R. B de Andrade, G. P. Rodrigues, G. F. Bauerfeldt, E. Ventura, M. Barbatti, S. A. do Monte, *J. Chem. Theory Comput.* **2018**, *14*, 4844. https://doi.org/10.1021/acs.jctc.8b00457.
[5] V. C. de Medeiros, R. B de Andrade, E. F. V. Leitão, E. Ventura, G. F. Bauerfeldt, M. Barbatti, S. A. do Monte, *J. Am. Chem. Soc.* **2016**, *138*, 272. https://doi.org/10.1021/jacs.5b10573.
[6] V. C. de Medeiros, S. A. do Monte, E. Ventura, *RSC Adv.* **2014**, *4*, 64085. https://doi.org/10.1039/C4RA10567B.
[7] G. P. Rodrigues, E. Ventura, S. A. do Monte, M. Barbatti, *J. Phys. Chem. A* **2014,** *118*, 12041. https://doi.org/10.1021/jp507681g.
[8] G. P. Rodrigues, J. R. Lucena Jr., E. Ventura, S. A. do Monte, I. Reva, R. Fausto, *J. Chem. Phys.* **2013,** *139*, 204302. https://doi.org/10.1063/1.4832376.
[9] V. C. de Medeiros, E. Ventura, S. A. do Monte, *Chem. Phys. Lett.* **2012**, *546*, 30. https://doi.org/10.1016/j.cplett.2012.07.037.
[10] J. R. Lucena Jr., E. Ventura, S. A. do Monte, R. C. M. U. Araújo, M. N. Ramos, *J. Chem. Phys.* **2007**, *127*, 164320. https://doi.org/10.1063/1.2800020.
[11] S. R. Langhoff, E. R. Davidson, *Int. J. Quantum Chem.* **1974**, *8*, 61. https://doi.org/10.1002/qua.560080106.

[12] P. J. Bruna, S. D. Peyerimhoff, R. J. Buenker, *Chem. Phys. Lett.* **1980**, *72*, 278. https://doi.org/10.1016/0009-2614(80)80291-0.

[13] A. Bunge, *J. Chem. Phys.* **1970**, *53*, 20. https://doi.org/10.1063/1.1673766.

[14] Shepard R, Shavitt I, Pitzer RM, Comeau DC, Pepper M, Lischka H, Szalay PG, Ahlrichs R, Brown FB, Zhao J (1988) A Progress Report on the Status of the COLUMBUS MRCI Program System. Int J Quantum Chem 34: 149−165. https://doi.org/10.1002/qua.560340819.

[15] Lischka, H.; Shepard, R.; Shavitt, I.; Pitzer, R. M.; Dallos, M.; Müller, T.; Szalay, P. G.; Brown, F. B.; Ahlrichs, R.; Böhm, H. J.; et al. COLUMBUS, an Ab Initio Electronic Structure Program, Release 7.0. www.univie.ac.at/columbus (accessed November 30, 2019).

[16] Lischka H, Shepard R, Pitzer RM, Shavitt I, Dallos M, Müller T, Szalay PG, Seth M, Kedziora GS, Yabushita S, Zhang Z. *Phys. Chem. Chem. Phys*. **2001**, *3*, 664. https://doi.org/10.1039/B008063M.

[17] Lischka H, Shepard R, Brown FB, Shavitt I (1981) New Implementation of the Graphical Unitary-Group Approach for Multi-Reference Direct Configuration-Interaction Calculations. Int J Quantum Chem 20: 91−100. https://doi.org/10.1002/qua.560200810.

[18] Helgaker T, Jensen H. J Aa,Jørgensen P, Olsen J, Ruud K, Ågren H, Andersen T, Bak KL, Bakken V, Christiansen O, et al. DALTON, an Ab Initio Electronic Structure Program, Release 1.0. 1997.

[19] T. H. Dunning, *J. Chem. Phys.* **1989**, *90*, 1007. https://doi.org/10.1063/1.456153.

[20] R. A. Kendall, T. H. Dunning, R. J. Harrison, *J. Chem. Phys.* **1992**, *96*, 6796. https://doi.org/10.1063/1.46256.

[21] D. E. Woon, T. H. Dunning. *J. Chem. Phys.* **1993**, *98*, 1358.https://doi.org/10.1063/1.464303 .

[22] M. N. R. Ashfold, G. A. King, D. Murdock, M. G. D. Nix, T. A. A. Oliver, A. G. Sage, *Phys. Chem. Chem. Phys*. **2010**, *12*, 1218.https://doi.org/10.1039/B921706A.

[23] L. Zhang, D. G. Truhlar, S. Sun, *Phys. Chem. Chem. Phys*. **2018**, *20*, 28144.https://doi.org/10.1039/C8CP05215H.

[24] H. S. You, S. Han, J. S. Lim, S. K. Kim, *J. Phys. Chem. Lett.* **2015**, *6*, 3202.https://doi.org/10.1021/acs.jpclett.5b01420.

[25] T. S. Venkatesan, S. G. Ramesh, W. Domcke, *J. Chem. Phys.* **2012**, *136*, 174312.https://doi.org/10.1063/1.4709608.

[26] Guang-Shuang-Mu Lin, C. Xie, D. Xie, *J. Phys. Chem. A* **2017**, *121*, 8432. https://doi.org/10.1021/acs.jpca.7b09070.

[27] H. Lischka, D. Nachtigallová, A. J. A. Aquino, P. G. Szalay, F. Plasser, F. B. C. Machado, M. Barbatti, *Chem. Rev.* **2018**, *118*, 7293.https://doi.org/10.1021/acs.chemrev.8b00244.

[28] S.A. do Monte, M. Dallos, T. Müller, H. Lischka, *Collect. Czech. Chem. Commun.* **2003**, *68*, 447.https://doi.org/10.1135/cccc20030447.